ARTICLE

OBC
www.rsc.org/obc

Conformational behavior of some hydroxamic acids

Rita Kakkar,* Rajni Grover and Preeti Chadha
Department of Chemistry, University of Delhi, Delhi-110 007, INDIA.
E-mail: rita_kakkar@vsnl.com

Received 16th January 2003, Accepted 6th May 2003
First published as an Advance Article on the web 19th May 2003

The conformational preferences of a few hydroxamic acids are investigated by the density functional B3LYP/6-311++G**//B3LYP/6-31G* and semiempirical AM1 and PM3 methods in this work. It is found that both semiempirical methods give satisfactory results in comparison with sophisticated DFT and *ab initio* calculations, except for the activation barriers, which are overestimated. Of the two semiempirical methods, while the PM3 method gives better results for relative stabilities, AM1 geometries are in slightly better agreement with the experiments. The keto forms are found to be most stable and the reaction pathways for the interconversion between the keto and enol forms have been deduced. The effect of solvation on the reaction has also been investigated, as has the effect of methyl substitution at the carbon and nitrogen atoms. All the investigated acids exhibit *N*-acid behavior.

Introduction

Hydroxamic acids have many applications in chemistry, as they are iron chelators with therapeutic potential,[1,2] and are also specific enzyme inhibitors.[3] They also possess photochemical properties.[4] However, in spite of their various applications, they still remain one of the lesser well-characterized classes of organic compounds, because of the existence of various tautomers and rotamers. Several experiments and theoretical calculations have been performed on the simplest hydroxamic acid, formohydroxamic acid, but it is still not known with certainty which of the conformers is present in the gas and solution phases. The problem is exacerbated by the fact that the various forms differ in energy by small amounts and the relative energies are basis set dependent in *ab initio* calculations. Further, the assignment of the correct structure to hydroxamate ions is also controversial and it is not known with certainty whether they are *N*-acids or *O*-acids in the gas phase and in aqueous solution.

In view of the diverse results obtained from previous calculations and experimental observations,[5–27] we have carried out a systematic study of the structures of various primary and secondary hydroxamic acids: -RCONR′OH; R = H, CH_3, C_2H_5; R′ = CH_3 (formo-, aceto-, propano- and *N*-methylacetohydroxamic acids). We have determined the relative acidities and stable configurations and tautomers of the neutral and deprotonated hydroxamic acids, that can serve as model hydroxamic acids used in cancer drug design, since these acids contain the smallest unit C=ONH that can bind to the DNA helix. The results of our density functional (DFT) calculations are also compared with semiempirical calculations at the AM1 and PM3 levels, with a view to deciding which method is suitable for studies on higher analogues for which accurate DFT and *ab initio* calculations are not possible because of their large size. Formohydroxamic acid, being a small system, has been studied at various levels of sophistication and should serve as a benchmark for quantum mechanical calculations on similar systems. The dependence on the basis set size was also investigated in this work.

Experimental

Computational details

We have first carried out calculations on the relative stabilities of the various tautomeric forms of formohydroxamic acid and then studied the reaction paths leading from one to the other. Calculations were then repeated for formohydroxamic acid in aqueous solution to see the effect of solvent on the relative stabilities and rotational barriers. Similar calculations were performed for the formohydroxamate anion to decide whether formohydroxamic acid is an *N*-acid or an *O*-acid. Formohydroxamic acid was then substituted to give the higher analogues, aceto-, propano- and *N*-methylacetohydroxamic acids. The same study was carried out with the new molecules to understand the effect of methyl substitution.

Quantum mechanical calculations at the semiempirical Austin Model 1, AM1[28] and Parametric Method 3, PM3[29,30] SCF levels were performed to examine the conformations in the gas phase using the MOPAC 7.0 program system.[30–32] The molecular geometries were fully optimized with respect to the energy without any conformational or symmetry restrictions. In the MOPAC calculations, the keywords PRECISE and GNORM = 0.01 were used in all geometry optimizations. This ensured that, in most cases, a mean gradient value lower than 0.01 kcal mol^{-1} $Å^{-1}$ was achieved. The vibrational frequencies were calculated to verify that the calculated structures are energy minima on the potential energy surface. Transition state structures were optimized using the eigenvalue following algorithm (keyword TS). In this case, the vibrational frequencies were determined to confirm the existence of one and only one negative eigenvalue.

Starting with these structures, the DFT method was used to estimate the relative conformational stabilities and the harmonic vibrational frequencies. The DFT calculations were performed with the B3LYP three-parameter density functional, which includes Becke's gradient exchange correction[33] and the Lee–Yang–Parr correlation functional.[34,35]

The geometries of all conformers, products and transition states were fully optimized at the B3LYP/6-31G* level of theory. This was followed by harmonic frequency calculations at this level. Single-point calculations were then performed at the B3LYP/6-311++G** level of theory for the geometries optimized at the B3LYP/6-31G* level of theory. The SCF = Tight option was used in these calculations, performed using Gaussian 98 Revision-A.11.2.[36] The calculated B3LYP/6-31G* vibrational frequencies were used to confirm all stationary point structures and to account for the zero-point vibrational energy contribution, which was scaled[37] down by a factor of 0.9804 and the vibrational frequencies were scaled by a factor of 0.9613.

DOI: 10.1039/b300466j

Aqueous phase calculations. The influence of solvation on the relative stability of conformers was studied at two levels: firstly by considering the effect of a single water molecule, and secondly by examining the effect of bulk solvent. The influence of bulk solvent was studied by the COSMO (COnductor-like Screening MOdel) procedure[38] implemented in MOPAC 7.0, with the dielectric constant (ε) taken as 78.39 for water at 298.15 K. The geometries were fully optimized with respect to the energy. For the sake of uniformity, the same model[39] (keyword SCRF = CPCM) was used in the density functional calculations. Again, the geometries were optimized with the 6-31G* basis set and single point calculations for the relative energies were performed with the 6-311++G** basis set.

Results and discussion

All the systems may exist in three tautomeric forms, *viz*., two rotamers of the keto form (**1*E***, **1*Z***), two rotamers of the iminol form (**2*E***, **2*Z***) and one charge-separated iminol form, **3**. The various forms and their interconversions are depicted in Fig. 1 where we have followed the notation of Wu and Ho.[5] For all the molecules, all stationary points, including transition states, were located, and the results are stated moleculewise in the following sections.

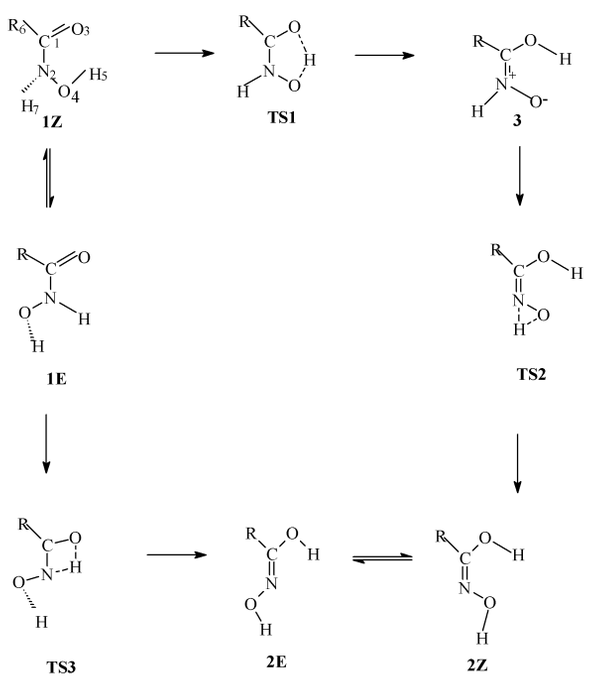

Fig. 1 The tautomeric forms of hydroxamic acids (R = H, CH_3, C_2H_5) and the transition states interconnecting them.

Formohydroxamic acid

Relative energies. Several theoretical calculations have been performed related to its structural analysis.[5–10] Bauer and Exner[11] reported that for the neutral molecule the keto forms, **1*E*** and **1*Z***, are favored over the iminol forms, **2*E*** and **2*Z***. Although low-level *ab initio* calculations suggested that the *E* tautomer exists preferentially in the gas phase, this preference was reduced at more sophisticated theoretical levels, and the *Z* structures became important when correlation energy was included.[5,8] Theoretical studies by Remko *et al*.[6] also implied that **1*Z*** is the most stable tautomer. Wu and Ho[5] examined the interconversion of the isomeric tautomers of formohydroxamic acid *via* intramolecular proton transfer by *ab initio* theoretical calculation, and found that the order of gas phase stability is **1*Z*** > **2*Z*** > **1*E*** > **2*E***. Experimental studies on the structure of formohydroxamic acid using X-ray[12] and ^{17}O NMR[13] confirmed that the most stable structure is **1*E*** in crystalline form and **1*Z*** in solution.

Table 1 DFT relative energies, and AM1 and PM3 heats of formation (kcal mol^{-1}) of the various stationary points on the gas phase formohydroxamic acid potential energy surface

System[a]	6-31G*	6-311++G**	AM1	PM3
1*Z*	0.0[b]	0.0[c]	−48.68	−47.39
1*E*	0.49	0.64	−49.44	−48.67
2*Z*	3.90	2.36	−51.00	−42.38
2*E*	7.09	5.80	−46.81	−43.44
3	14.58	13.00	−30.64	−32.01
TS1	14.68	13.79	−7.03	−7.96
TS2	54.62	53.45	20.36	25.85
TS3	43.15	43.40	8.87	−0.45
1a-*cis*	368.48	344.17	−51.35	−51.02
1a-*trans*	364.05	349.01	−58.52	−60.62
1b	353.44	341.07	−66.81	−66.51
1c	383.94	366.82	−61.67	−53.45

[a] See Figs. 1 and 2. [b] ZPVE corrected energy: −244.994263 hartrees. [c] ZPVE corrected energy: −245.087041 hartrees.

The calculated relative energies for the tautomers and rotamers, fully optimized at the B3LYP/6-31G*//B3LYP/6-31G*, B3LYP/6-311++G**//B3LYP/6-31G*, AM1 and PM3 levels, are listed in Table 1. Among the five forms, the charge-separated structure **3** is calculated to be the least stable, as expected. The DFT order of stabilities is **1*Z*** > **1*E*** > **2*Z*** > **2*E*** > **3**. Both basis sets give similar results for the stability order. Thus, the keto tautomers are preferred over the iminol ones. Amongst the two rotamers, the finding that **1*Z*** is more stable than **1*E*** agrees with the expectation based on the possibility of stabilization of **1*Z*** due to intramolecular hydrogen bonding (see Fig. 1). Besides, the calculated smaller dipole moment of **1*Z*** (3.00 D compared to 3.37 D of **1*E***) also agrees with the finding[14,15] that the rotamer with the smaller dipole moment is always more stable. However, the difference in energy between the **1*Z*** and **1*E*** rotamers is not much, and we may conclude that **1*Z*** and **1*E*** coexist in the gas phase. From the calculated values of the gas phase free energies of the **1*Z*** and **1*E*** forms, we find that at 298.15 K and 1 atmosphere pressure, the free energy difference is 0.6 kcal mol^{-1}, which implies that **1*Z*** is present to the extent of ~75%, according to the equation $\Delta G = -RT \ln K$. However, none of the two semiempirical methods predicts the correct order of stabilities. According to AM1, the most stable structure is **2*Z*** (stabilities **2*Z*** > **1*E*** > **1*Z*** > **2*E***), whereas the PM3 method suggests that the stability of **1*E*** is greater than that of any other tautomer (stabilities **1*E*** > **1*Z*** > **2*E*** > **2*Z***). Of the two methods, the PM3 results for energies are closer to DFT predictions, since it predicts greater stability for the keto forms.

Geometries. The two keto forms (**1*Z*** and **1*E***) are nonplanar, whereas the two iminol forms, **2*E*** and **2*Z***, are nearly planar. In Table 2, we report the calculated optimized geometries for **1*E***, calculated by the three methods, as well as the experimentally determined geometries. This form has been chosen for comparison, as X-ray crystallography data are available for only this form. The DFT results are in good agreement with experimental results. Of the two semiempirical methods, the AM1 geometries are in slightly better agreement with the experiments.

Intramolecular proton transfer. We also calculated the potential energy profiles for the reaction paths for intramolecular proton transfer of formohydroxamic acid tautomers, as shown in Fig. 1. The relative energies of the transition states are reported in Table 1. The first reaction considered was the transformation of **1*Z*** to **3** *via* the transition state, TS1. The calculated activation energies for the transformation of **1*Z*** to **3** are 14.7 and 13.8 kcal mol^{-1}, respectively, for the 6-31G* and

Table 2 Optimized geometries of **1*E*** (bond lengths in Ångstroms; bond angles in degrees) in the gas phase and in solution

	DFT		AM1		PM3		
	Gas	Solution	Gas	Solution	Gas	Solution	Expt.[a]
N_2–C_1	1.382	1.351	1.418	1.400	1.439	1.418	1.312
O_3–C_1	1.213	1.253	1.236	1.254	1.212	1.227	1.257
O_4–N_2	1.411	1.428	1.333	1.332	1.442	1.440	1.388
H_5–O_4	0.972	0.997	0.978	0.983	0.949	0.952	0.86
H_6–C_1	1.105	1.099	1.112	1.113	1.102	1.100	1.01
H_7–N_2	1.018	1.027	1.013	1.014	0.995	0.993	0.91
$O_3C_1N_2$	123.3	124.0	120.5	119.3	117.2	116.3	125.3
$O_4N_2C_1$	115.4	118.4	114.0	115.2	112.5	113.9	118.3
$H_5O_4N_2$	103.9	106.1	105.4	106.1	101.2	101.5	111
$H_6C_1N_2$	111.5	112.6	114.8	117.0	118.4	120.3	113
$H_7N_2C_1$	115.6	124.4	114.7	117.3	116.7	118.2	123
$O_4N_2C_1O_3$	158.9	172.1	156.0	162.4	155.3	161.0	
$H_5O_4N_2C_1$	117.1	101.1	110.0	95.9	112.5	104.3	
$H_6C_1N_2O_4$	−24.3	−8.7	−29.3	−23.5	−29.2	−24.2	
$H_7N_2C_1O_3$	26.4	8.5	27.7	29.7	32.5	34.8	

[a] From reference 12.

6-311++G** basis sets (41.7 and 39.4 kcal mol^{-1} at the AM1 and PM3 levels, respectively). The transformation of **3** to **2*Z*** occurs *via* another transition state, TS2, which has an even higher energy, and the calculated activation energies for this step are 40.0 and 40.5 kcal mol^{-1}, respectively, with the 6-31G* and 6-311++G** basis sets. At the AM1 and PM3 levels, the values are, respectively, 51.0 and 57.9 kcal mol^{-1}. Again the semiempirical methods grossly overestimate the barriers. However, there is close agreement between our calculated DFT results with both basis sets and the *ab initio* G2 results.[5] This confirms the accuracy of DFT calculations, which can be performed at a fraction of the cost of the high level G2 calculations.

Another pathway considered here is the transformation of **1*E*** to **2*E*** *via* the transition state TS3. This path was found to have an activation energy of 43.2 and 43.4 kcal mol^{-1}, respectively, with the 6-31G* and 6-311++G** basis sets. The AM1, PM3 and G2[5] barriers are found to be 57.6, 46.9 and 42.4 kcal mol^{-1}, respectively, and our calculated values agree with the G2 values. The energies of the transition states reflect their different respective ring strains, and the energy order is TS2 > TS3 > TS1, since the three transition states involve three, four and five membered rings, respectively. Hence, of the two possible pathways for the transformation of the keto form (**1*Z***) to the enol form (**2*Z***, see Fig. 1), the first pathway, *i.e.* **1*Z*** ⟶ **3** ⟶ **2*Z***, involves the highly strained three-centered transition state (TS2) and does not seem likely. The second pathway, **1*Z*** ⟶ **1*E*** ⟶ **2*E*** ⟶ **2*Z***, involves the relatively less strained four-center-like transition state, TS3, and should be thus preferred.

The intramolecular proton transfer in hydroxamic acid has been studied by Wu and Ho,[5] where they discussed the detailed transformation from the keto form (**1*Z***) to the enol form (**2*Z***). Our findings agree with theirs. However, there is a substantial barrier to the rotation of **2*E*** to **2*Z***, which they did not take into account in their discussion. At the B3LYP/6-311++G**//B3LYP/6-31G* level, which is the level discussed in the rest of the paper, as the 6-31G* basis set fails to describe the small differences in energies of the tautomers satisfactorily, the barrier is 45.2 kcal mol^{-1}, which is much higher than the general rotational barrier for CN bonds, which is in the range 10–15 kcal mol^{-1}.[16] This is to be expected, as the CN bond is a double bond in this case. In fact, the transition state has a higher energy (51.0 kcal mol^{-1}) than TS1 and TS3. Even at the AM1 and PM3 levels, the rotational barrier is found to be significant (38.8 kcal mol^{-1} with AM1), but its energy is smaller than that of TS3, and so the overall barrier is not affected. Wu and Ho[5] had not calculated this rotational barrier, assuming it to be the normal 10–15 kcal mol^{-1},[16] and hence smaller than the barrier separating **1*E*** and **2*E*** *via* a hydrogen shift. However, as we have seen, this barrier is not negligible, and it is quite likely that the **2*E*** tautomer formed initially (with an activation energy of 43.4 kcal mol^{-1}) does not undergo subsequent isomerization to the more stable rotamer, **2*Z***. The rotational barrier separating **1*Z*** and **1*E*** is, however, much smaller (17.3 kcal mol^{-1}). The overall activation energies for the two pathways are 53.5 and 51.0 kcal mol^{-1} (69.0 and 57.6 kcal mol^{-1} at the AM1 level, and 73.2 and 46.9 kcal mol^{-1} at the PM3 level), and the latter is only slightly preferred.

Intermolecular hydrogen bonding. We have also carried out B3LYP/6-311++G**//B3LYP/6-31G* calculations on the monohydrate of formohydroxamic acid to see the role of hydrogen bonding with water molecules on the relative stabilities in solution. We have therefore considered the two monohydrates of the **1*Z*** and **1*E*** forms of formohydroxamic acid.

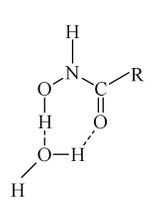

1Z.H$_2$O

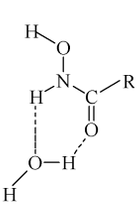

1E.H$_2$O

1*Z*·H$_2$O is found to be more stable than **1*E*·H$_2$O** by 2.5 kcal mol^{-1} (ZPVE corrected energies −321.5366173 and −321.5325913 hartrees, respectively). Thus, **1*Z*** becomes more strongly favored in aqueous solution. The calculated enthalpies for **1*Z***, **1*E*·H$_2$O**,, **1*Z*·H$_2$O** and **1*E*·H$_2$O** at 298.15 K and 1 atmosphere pressure are, respectively, −245.0808350, −245.0797015, −76.4334739, −321.5275095 and −321.5232253 hartrees. Thus, the reaction enthalpy for the process

$$\mathbf{1}Z + H_2O \longrightarrow \mathbf{1}Z\cdot\mathbf{H_2O}$$

is calculated as −8.3 kcal mol^{-1} and that for

$$\mathbf{1}E + H_2O \longrightarrow \mathbf{1}E\cdot\mathbf{H_2O}$$

is −6.3 kcal mol^{-1}. Thus, hydrogen bonding with water stabilizes **1*Z*** to a greater extent than **1*E***. The enthalpies were estimated by adding the thermal corrections to the energy

to account for translational, vibrational and rotational motion at 298.15 K and 1 atmosphere pressure.

The AM1 heats of formation of the **1*Z*·H$_2$O** and **1*E*·H$_2$O** complexes are, respectively, −113.9 and −114.8 kcal mol^{-1} for formohydroxamic acid, −120.4 and −121.3 kcal mol^{-1} for acetohydroxamic acid, and −125.3 and −127.8 kcal mol^{-1} for propanohydroxamic acid. Thus, one water molecule does not have any marked effect on the order of stabilities, and the **1*E*** form remains slightly preferred according to AM1. However, further solvation of the monohydrate reverses the stability order, as the heats of formation of **1*Z*·H$_2$O** and **1*E*·H$_2$O** in aqueous solution are −132.5 kcal mol^{-1} and −131.9 kcal mol^{-1}, respectively, for formohydroxamic acid.

Aqueous phase calculations. The effect of bulk water was considered by calculating the free energies of the various tautomers in aqueous solution (see Table 3), and it was found that the values for **1*E***, **2*Z*** and **2*E*** are 7.5, 5.0 and 7.2 kcal mol^{-1} relative to the **1*Z*** form at 298.15 K and 1 atmosphere pressure (see Table 3). Thus, the **1*Z*** form becomes more emphatically favored in aqueous solution, in agreement with experimental results,[13] and the iminol forms also become apparent (stability order: **1*Z*** > **2*Z*** > **2*E*** > **1*E***). The semiempirical methods also favor this form in aqueous solution, and the AM1 order of stabilities is **1*Z*** > **1*E*** > **2*Z*** > **2*E***. The PM3 order of stabilities is **1*Z*** > **1*E*** > **2*E*** > **2*Z*** (see Table 3). The AM1 relative energies are in slightly better agreement with DFT than the PM3 values.

The optimized geometries for the **1*E*** form in solution are also given in Table 2. It can be seen that aqueous solvation reduces the C–N bond length considerably (by ~0.03 Å). There is a concomitant increase in the carbonyl bond length (~0.04 Å), signifying that delocalization of electrons takes place from the carbonyl bond to the carbon–nitrogen bond. The N–C and C=O stretching frequencies increase by 39 cm^{-1} and decrease by 174 cm^{-1}, respectively (see Table 4). The carbonyl oxygen is also involved in intermolecular hydrogen bonding with water molecules. The variation in the C–N, O–N and O–C bond lengths in the isolated molecule with one complexed water and in the bulk water environments for the two rotamers is interesting. Table 4 shows that solvation in **1*Z*** considerably reduces the C–N and O–N bond lengths, but lengthens the C–O bond only slightly. For **1*E***, however, it is the C–O bond that shows the largest increase. In both cases, while the other two bonds show a constant increase or decrease in going from the isolated molecule to a complex with a single water molecule and then to bulk water, the O–N bond is shortest in the single water molecule complex, accounting for the destabilization.

Table 3 B3LYP/6-311++G**//B3LYP/6-31G* relative free energies, and AM1 and PM3 heats of formation (kcal mol^{-1}) at 298.15 K and 1 atmosphere pressure of the various stationary points on the aqueous phase formohydroxamic acid potential energy surface

System	DFT	AM1	PM3
1*Z*	0.0[a]	−65.51	−62.33
1*E*	7.51	−64.72	−60.52
2*Z*	5.04	−61.95	−53.27
2*E*	7.18	−57.84	−54.30
3		−56.12	−58.15
TS1		−28.73	−30.90
TS2		1.10	9.06
TS3		−5.78	−13.65
1a-*cis*		−152.94	−156.12
1a-*trans*		−153.39	−158.84
1b		−155.33	−157.39
1c		−151.58	−146.56

[a] G_{soln} = −245.155619 hartrees.

Anions. As mentioned in the Introduction, the relative stabilities of the anions are also not known with certainty. Since the **1*Z*** form seems to be the favored one in the gas phase and in aqueous solution, dissociation could occur either from the NO–H group leading to the anion **1a**, both *cis* and *trans* forms of which are possible, making formohydroxamic acid an *O*-acid. However, if the N–H proton were to dissociate, it would be an *N*-acid, leading to the anion **1b**. In addition, there is a possibility of dissociation from the NO–H group of the almost equally stable **1*E***, leading to structure **1c**, making formohydroxamic acid an *O*-acid (see Fig. 2).

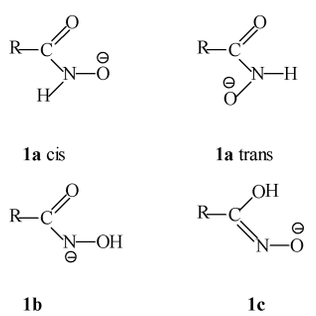

Fig. 2 Possible anion structures.

We have carried out a study of the relative stabilities of the possible anions, and the results are presented in Table 1. All methods predict that the **1b** anion is the most stable, followed by **1a**-*cis*, **1a**-*trans* and **1c** in that order in the case of DFT. The finding that **1b** is more stable than the other anions agrees with high-level *ab initio*[7,17] calculations. The greater stability of **1b** over **1a**-*cis*, both of which are derived from **1*Z***, can be easily explained. In the former, an electron resonance involving the N–C=O bonds is possible, which should stabilize the two unshared electron pairs on the nitrogen atom. That this occurs is confirmed by the following: the C–N bond length in **1b** decreases to 1.318 Å from 1.361 Å in **1*Z*** (see Table 4), and its vibrational frequency also increases by 56 cm^{-1}. Similarly, the carbonyl bond length increases to 1.276 Å compared to 1.225 Å in **1*Z***; its vibrational frequency also reduces by 96 cm^{-1} (see Table 4). The calculated AM1 C–N and C=O bond orders are also 1.523 and 1.418, respectively. This implies that a resonance exists between the keto and iminol forms, as shown below:

Table 4 Variation in bond lengths and stretching frequencies on solvation for the two rotamers of the keto form and the anion

Bond length	**1*Z***	**1*Z*·H$_2$O**	**1*Z*** (aq.)	**1*E***	**1*E*·H$_2$O**	**1*E*** (aq.)	**1b**
CN	1.361	1.347	1.342	1.382	1.361	1.351	1.318
ON	1.405	1.389	1.398	1.411	1.406	1.428	1.461
OC	1.225	1.230	1.234	1.213	1.227	1.253	1.276
Stretching frequencies							
CN	1165	1210	1187	1201	1251	1240	1221
OC	1706	1710	1665	1755	1668	1581	1610

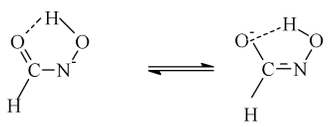

1b

keto iminol

IR studies[18] also show a red shift in the carbonyl frequency, indicating that it is in resonance with the nitrogen lone pairs. From the calculated partial atomic charges on the various atoms in **1*Z*** and **1b** (see Table 5), it is seen that the largest increase in negative charge occurs at the carbonyl oxygen, followed by the change at the nitrogen on formation of the anion **1b** from **1*Z***. This again supports the concept of resonance in the anion, as the deprotonated formohydroxamic acid may be considered as the nitrogen-deprotonated keto form, or, alternatively, the *C*-hydroxy oxygen-deprotonated iminol form.

In contrast, if the proton dissociates from the oxygen atom to form **1a**-*cis*, no such electron resonance effect develops to stabilize the anion. Instead, the originally existing intramolecular hydrogen bonding also disappears, and hence this increases the instability of the resultant anion. The greater stability of **1b** implies that formohydroxamic acid is an *N*-acid in the gas phase, and this is in accord with most experimental and theoretical conclusions.[5,6] The calculated proton dissociation free energy for formohydroxamic acid is 347.4 kcal mol^{-1}. This was calculated from the relation $G_{anion} + G_{proton} - G_{1Z}$, where the respective terms are the free energies of the **1b** anion, the proton (0.01 hartrees) and the undissociated **1*Z*** form, estimated after making the required thermal corrections to the energy arising from the translational, rotational and vibrational motions at 298.15 K and 1 atmosphere pressure. However, it may be mentioned that, as the three forms **1*Z***, **1*E*** and **2*Z*** are in equilibrium in the gas phase, it may also be considered as an *O*- acid as a result of deprotonation from the oxygen of the **2*Z*** form. This is supported by the structure of the anion, which is a resonance hybrid of the two forms.

Wu and Ho[5] have also argued for *N* acid behaviour of hydroxamic acids thus: since structure **1*Z*** is the most stable conformation of formohydroxamic acid in the aqueous phase, its acidity would depend on which hydrogen atom (attached to the *N* atom or the *O* atom) can be dissociated easily. Since the barrier to the transformation **1*Z*** ⟶ **3** is smaller than that for the intramolecular proton transfer (**1*Z*** ⟶ **1*E*** ⟶ **2*E*** ⟶ **2*Z***), the former reaction takes place faster and the proton on O_4 (H_5) is not available for dissociation, as it remains between the two oxygens, O_4 and O_3. The **1*Z*** to **2*Z*** transformation, which involves the transfer of the proton (H_7) attached to N_2, however, is more difficult and thus this proton is relatively easy to dissociate.

Aceto- and propanohydroxamic acids

The next two higher homologues of formohydroxamic acid are aceto- and propanohydroxamic acids. The former is best known as Lithostat, a drug used in the cure of kidney ailments, although its side effects include haemolytic anaemia, blood clotting and headaches. Fishbein and Carbone[19] first reported its function as an inhibitor of the enzyme urease. Recently, a theoretical and experimental study of the solvent effect on its protonation has been carried out.[20]

A similar trend in energy is observed in the case of these two molecules, with the energy gap between the **1*E*** and **1*Z*** forms becoming smaller with each substitution (see Table 6), until for propanohydroxamic acid, the **1*E*** form becomes favored over **1*Z***. The basis set dependence of the calculations is again reflected in the fact that calculations with the 6-31G* basis set favor the **1*Z*** isomer by 0.9 kcal mol^{-1}. X-ray crystallographic analysis of acetohydroxamic acid revealed the stable structure to be the **1*Z*** form in the solid state.[21] The greater stability of the **1*E*** form for propanohydroxamic acid in the gas phase seems contrary to the fact that an intramolecular hydrogen bond in the **1*Z*** form is disabled in the **1*E*** form. However, the small differences in energy suggest that both aceto- and propanohydroxamic acids exist in the **1*Z*** and **1*E*** forms that are in equilibrium in the gas phase. This prediction is consistent with previous *ab initio* calculations.[22]

Table 5 Calculated change in the partial atomic charges on the various atoms on formation of the anion **1b** from **1*Z*** for formohydroxamic acid

Atom[a]	**1*Z***	**1b**	Δq
C_1	0.039	−0.083	−0.122
N_2	−0.147	−0.287	−0.140
O_3	−0.386	−0.558	−0.172
O_4	−0.167	−0.279	−0.112
H_5	0.261	0.195	−0.066
H_6	0.120	−0.012	−0.132
H_7	0.281	—	—

[a] See Fig. 1 for the numbering of atoms. All calculations at the B3LYP/6-31++G**//B3LYP/6-31G* level.

As far as the activation barriers are concerned, since all methods agree that for formohydroxamic acid, the pathway from **1*Z*** to **2*E*** must involve only TS3, we have calculated the energy of only this transition state. For the gas phase, the overall barriers are 43.4, 40.8 and 39.0 kcal mol^{-1}, respectively, for formo-, aceto- and propanohydroxamic acids (AM1: 57.6, 56.5 and 56.3 kcal mol^{-1}, PM3: 46.9, 47.3 and 47.2 kcal mol^{-1}). The barriers decrease slightly with every methyl substitution.

The relative energies of the anions are also given in Table 6. The observation that **1b** is the most stable form agrees well with high-level *ab initio* and density functional calculations.[22] Decouzon *et al.*[23] measured gas phase acidities of acetohydroxamic acid as well as those of its *N*-methyl and *O*-methyl derivatives, concluding that it behaves essentially as an *N*-acid in the gas phase. Our calculated value for the proton dissociation free energy of acetohydroxamic acid (337.1 kcal mol^{-1}) agrees well with their value (339.1 ± 2 kcal mol^{-1}). For propanohydroxamic acid, the calculated value is 335.3 kcal mol^{-1}. Other authors[7,17,24] also confirmed *N*-acid behavior for hydroxamic acids in gas phase and in DMSO solution, and *O*-acid character in aqueous solution.

N-methylacetohydroxamic acid

In contrast to the situation for the above acids, in *N*- substituted derivatives, there is no possibility of the enol form as the nitrogen lacks a hydrogen atom for transfer to the carbonyl oxygen. In this case, too, we found that, like propanohydroxamic acid, the **1*Z*** form is less stable than the **1*E*** form by 0.8 kcal mol^{-1} (see Table 6). However, the small difference suggests that both forms are in equilibrium in the gas phase. For the anion, it is found that the **1a**-*trans* form is more stable than the **1a**-*cis* form by 10.9 kcal mol^{-1} (see Table 6). This agrees with the prediction of previous *ab initio* calculations.[22] The calculated proton dissociation energy (343.4 kcal mol^{-1}) agrees with the experimental value[23] of 346.9 ± 2 kcal mol^{-1}.

Barriers to rotation. The reaction scheme shown in Fig. 1 entails rotations about the C–N bond for the interconversion between the two pairs of rotational isomers **1*Z***, **1*E*** and **2*Z***, **2*E***. While the latter barrier is quite high, the smaller barrier to the CN rotation from **1*Z*** to **1*E*** was not taken into consideration for the above discussion, but it does play an important role in metal chelation. The substituents at nitrogen and carbon can modify the *cis* : *trans* (*Z* : *E*) ratio, as was found for a series of monohydroxamic acids.[25,26] As the required conformation for the

Table 6 DFT relative energies and AM1 and PM3 heats of formation (kcal mol^{-1}) of the various stationary points on the acetohydroxamic acid and propanohydroxamic acid potential energy surfaces

	Aceto-			Propano-			*N*-methylaceto-		
System	DFT	AM1	PM3	DFT	AM1	PM3	DFT	AM1	PM3
1*Z*	0.0[a]	−55.28	−56.60	0.0[b]	−61.11	−60.68	0.0[c]	−48.66	−57.04
1*E*	1.45	−55.45	−56.84	−0.96	−61.19	−60.95	−0.82	−49.23	−57.38
2*Z*	3.82	−55.59	−49.98	2.67	−60.49	−53.06	—	—	—
2*E*	6.19	−52.89	−51.74	5.02	−58.08	−55.07	—	—	—
TS3	40.84	1.22	−9.27	38.95	−4.80	−13.48	—	—	—
1a-*cis*	356.50	−57.27	−60.01	353.73	−63.29	−64.84	360.45	−50.42	−58.62
1a-*trans*	350.86	−63.62	−68.45	348.30	−70.15	−72.97	349.57	−57.08	−66.95
1b	343.38	−71.39	−76.53	341.59	−78.06	−79.37	—	—	—
1c	413.03	−69.55	−62.76	366.95	−75.36	−67.73	—	—	—

[a] ZPVE corrected energy = −284.3956842 hartrees. [b] ZPVE corrected energy = −323.6880154 hartrees. [c] ZPVE corrected energy = −323.6882328 hartrees.

formation of a normal (*O*,*O*) chelate is *cis*-(*Z*), correlation between the *Z* : *E* ratio and the stability of the chelate (both thermodynamic and kinetic), can be expected.

Metal complexation utilizing the normal (*O*,*O*) mode of hydroxamate-metal coordination requires initial formation of the *Z*-conformer and overcoming any *E*-rotational barrier. As we have seen, in most cases, both conformers co-exist at room temperature. The effects of this barrier are also reflected in kinetic parameters obtained from the sequestration of iron by hydroxamic acids from the polynuclear iron complex, $[Fe_{11}O_6(OH)_6(O_2CPh)_{15}]$.

For formohydroxamic acid, the calculated rotational barriers in the gas phase and in aqueous solution are, respectively, 17.9 and 20.2 kcal mol^{-1}, respectively. For acetohydroxamic acid, the gas phase barrier is calculated as 16.7 kcal mol^{-1}. Thus, the rotational barriers increase on aqueous solvation. Although the MP2/6-311G** calculations[27] predict otherwise, the rotational barriers decrease with increasing methyl substitution for the gas phase. Part of the discrepancy between our results and those of Brown *et al.*[27] arises from the underestimation of the stability of the *Z* form in their calculations, due to the non-inclusion of diffuse functions, that could lead to an incorrect description of hydrogen bonding effects. For *N*-methyl acetohydroxamic acid, the calculated rotational barrier from the more stable **1***E* form is 16.6 kcal mol^{-1}, as compared with a value of 16.0 kcal mol^{-1} from MP2/6-311G** calculations.[27]

Conclusions

Our calculations on the various systems related to hydroxamic acids reveal the following: the 6-31G* basis set is inadequate for describing these highly polar systems, and diffuse and polarization functions must be included to account for the weak intramolecular interactions, and to properly describe the small differences in energy amongst the various tautomers. Comparison with our DFT calculations reveals that, of the two semiempirical methods, AM1 has a slight edge over PM3 as it predicts correct geometries and order of stabilities of the tautomers and the anions. The barrier to the rotation of **2***E* to the more stable rotamer, **2***Z*, is significant, and hence affects the activation energy for the transformation of **1***Z* to **2***Z*. The keto tautomer (**1**) is found to be more stable, both in the gas phase and in aqueous solution, for all the systems investigated. While generally the **1***Z* form seems to be preferred in the gas phase for the lower homologues, and **1***E* for the higher homologues, in solution, the **1***Z* form is preferred. The barrier to the interconversion between these two forms is of the order of 18 kcal mol^{-1}, but increases in aqueous solution. The energy gap between the **1***Z* and **1***E* forms decreases with increasing methyl substitution and so does the rotational barrier for the interconversion, implying that for the higher homologues, both forms are in equilibrium. In addition, the barrier to the interconversion of the keto and iminol forms decreases with each methyl substitution, making such interconversions possible. Both semiempirical methods overestimate energy barriers, but the AM1 method gives a slightly better description of the geometries and energy orders. It is unequivocally proved that proton dissociation occurs from the nitrogen atom, making these *N*-acids. It is also found that the proton dissociation free energies decrease with increasing methyl substitution. However, for the *N*-methyl derivative, the proton dissociation energy is higher because this is an *O*-acid as the nitrogen is substituted. There is a sizeable barrier to the interconversion of the two rotamers of the iminol form and this should affect the overall barrier to the interconversion of the *Z* forms of the keto and iminol tautomers.

Acknowledgements

Two of the authors (R. G. and P. C.) thank the Council of Scientific and Industrial Research (CSIR), New Delhi, for research fellowships.

References

1 B. Barlaam, P. Koza and J. Berriot, *Tetrahedron*, 1999, **55**, 7221–7232.
2 M. J. Miller, *Chem. Rev.*, 1989, **89**, 1563–1579 and references therein.
3 A. O. Stewart and J. G. Martin, *J. Org. Chem.*, 1989, **54**, 1221–1223.
4 E. Lipczyñska-Kochany, *Chem. Rev.*, 1991, **91**, 477–491.
5 D. -H. Wu and J. -J. Ho, *J. Phys. Chem. A*, 1998, **102**, 3582–3586.
6 M. Remko, P. Mach, P. v. R. Schleyer and O. Exner, *J. Mol. Struct.: THEOCHEM*, 1993, **279**, 139–150.
7 A. Bagno, C. Comuzzi and G. Scorrano, *J. Am. Chem. Soc.*, 1994, **116**, 916–924.
8 L. Turi, J. J. Dannenberg, J. Rama and O. N. Ventura, *J. Phys. Chem.*, 1992, **96**, 3709–3712.
9 M. Remko, *J. Phys. Chem. A*, 2002, **20**, 5005–5010.
10 C. M. R. Sant'Anna, *Quim. Nova*, 2001, **24**, 583–587.
11 L. Bauer and O. Exner, *Angew. Chem., Int. Ed. Engl.*, 1974, **13**, 376–384.
12 I. K. Larsen, *Acta Crystallogr., Sect. B: Struct. Sci.*, 1988, **44**, 527–533.
13 E. Lipczyñska-Kochany and H. Iwamura, *J. Org. Chem.*, 1982, **47**, 5277–5282.
14 K. B. Wiberg and K. E. Laidig, *J. Am. Chem. Soc.*, 1988, **110**, 1872–1874.
15 X. Wang and K. N. Houk, *J. Am. Chem. Soc.*, 1988, **110**, 1870–1872.
16 C. E. Blom and Hs. H. Günthard, *Chem. Phys. Lett.*, 1981, **84**, 267–271.
17 O. N. Ventura, J. B. Rama, L. Turi and J. J. Dannenberg, *J. Am. Chem. Soc.*, 1993, **115**, 5754–5761.
18 O. Exner, *Collect. Czech. Chem. Commun.*, 1964, **29**, 1337–1343.
19 W. N. Fishbein and P. P. Carbone, *J. Biol. Chem.*, 1965, **240**, 2407–2414.
20 B. Garcia, S. Ibeas, J. M. Leal, M. L. Senent, A. Niño and C. Muñoz-Caro, *Chem. Eur. J.*, 200, **6**, 2644–2652.

21 B. H. Bracher and R. W. H. Small, *Acta Crystallogr., Sect. B: Struct. Sci.*, 1970, **B26**, 1705–1709.
22 J. E. Yazal and Y. –P. Pang, *J. Phys. Chem. A*, 1999, **103**, 8346–8350.
23 M. Decouzon, O. Exner, J. –F. Gal and P. –C. Maria, *J. Org. Chem.*, 1990, **55**, 3980–3981.
24 F. G. Bordwell, H. E. Fried, D. L. Hughes, T. –Y. Lynch, A. V. Satish and Y. E. Whang, *J. Org. Chem.*, 1990, **55**, 3330–3336.
25 D. A. Brown, W. K. Glass, R. Mageswaran and S. Ali Mohammed, *Magn. Res. Chem.*, 1991, **29**, 40–45.
26 D. A. Brown, R. A. Coogan, N. J. Fitzpatrick, W. K. Glass, D. E. Abukshima, L. Shiels, M. Ahlgrén, K. Smolander, T. T. Pakkanen, T. A. Pakkanen and M. Peräkylä, *J. Chem. Soc., Perkin Trans. 2*, 1996, 2673–2679.
27 D. A. Brown, L. Cuffe, N. J. Fitzpatrick, W. K. Glass and K. Herlihy, *COST D8 & ESF workshop on 'Biological and medicinal aspects of metal speciation'*, JATE, Szeged, Hungary, 23–25 Aug., 1998.
28 M. J. S. Dewar, E. G. Zoebisch, E. F. Healy and J. J. P. Stewart, *J. Am. Chem. Soc.*, 1985, **107**, 3902–3909.
29 J. J. P. Stewart, *J. Comput. Chem.*, 1989, **10**, 209–264.
30 J. J. P. Stewart, *J. Comput.-Aided Mol. Des.*, 1990, **4**, 1–105.
31 J. J. P. Stewart, *J. Comput. Chem.*, 1990, **11**, 543–544.
32 J. J. P. Stewart, *QCPE Bull.*, 1990, **10**, 86.
33 A. D. Becke, *J. Chem. Phys.*, 1993, **98**, 5648–5652.
34 C. Lee, W. Yang and R. G. Parr, *Phys. Rev.*, 1988, **B 37**, 785–789.
35 B. Miehlich, A. Savin, H. Stoll and H. Preuss, *Chem. Phys. Lett.*, 1989, **157**, 200–206.
36 M. J. Frisch, G. W. Trucks, H. B. Schlegel, G. E. Scuseria, M. A. Robb, J. R. Cheeseman, V. G. Zakrzewski, J. A. Montgomery Jr., R. E. Stratmann, J. C. Burant, S. Dapprich, J. M. Millam, A. D. Daniels, K. N. Kudin, M. C. Strain, O. Farkas, J. Tomasi, V. Barone, M. Cossi, R. Cammi, B. Mennucci, C. Pomelli, C. Adamo, S. Clifford, J. Ochterski, G. A. Petersson, P. Y. Ayala, Q. Cui, K. Morokuma, N. Rega, P. Salvador, J. J. Dannenberg, D. K. Malick, A. D. Rabuck, K. Raghavachari, J. B. Foresman, J. Cioslowski, J. V. Ortiz, A. G. Baboul, B. B. Stefanov, G. Liu, A. Liashenko, P. Piskorz, I. Komaromi, R. Gomperts, R. L. Martin, D. J. Fox, T. Keith, M. A. Al-Laham, C. Y. Peng, A. Nanayakkara, M. Challacombe, P. M. W. Gill, B. Johnson, W. Chen, M. W. Wong, J. L. Andres, C. Gonzalez, M. Head-Gordon, E. S. Replogle, J. A. Pople,GAUSSIAN 98, Gaussian, Inc., Pittsburgh PA, 2001.
37 A. P. Scott and L. Radom, *J. Phys. Chem.*, 1996, **100**, 16502–16513.
38 A. Klamt and G. Schüürmann, *J. Chem. Soc., Perkin Trans. 2*, 1993, 799–805.
39 V. Barone and M. Cossi, *J. Phys. Chem.*, 1998, **A 102**, 1995–2001.